AMBIGUOUS PSI MEASUREMENTS

J. Duro[(1)], N. Miranda[(1)], G. Cooksley[(1)], E. Biescas [(1)], A. Arnaud [(1)]

[(1)] Altamira Information, C/ Còrcega 381-387, 2n 3a, E-8037 Barcelona, Spain,
Email: javier.duro@altamira-information.com

ABSTRACT

The Stable Point Network (SPN) is a persistent scatterer interferometric technique developed by ALTAMIRA INFORMATION in 2001. The technique makes use of both ERS SAR and/or ASAR differential phase measurements to generate long term terrain movement and precise height maps with the same resolution as the original SAR images. The algorithm is capable to use all the available phase information even in conditions of large baselines or platform instabilities giving place to large Doppler centroid variations. Such behaviour is handled by precise location estimate of the scatterer within the pixel and accurate elevation extraction which permits the exact location of the radar measurement in ground geometry. However not all the SPN interferometric measurements within a pixel have a direct correspondence in the real scene. Some points presented as measurement points may not be related to existing structures on ground but directly generated by the processing itself. For instance, several artifacts can be created in the Synthetic Aperture Radar images due to the signal acquisition system. Azimuth ambiguities are one of them. They may appears as strong targets in low backscattering areas like forest or water. Secondary lobes of strong targets are also an issue. Since low level signals can be masked by the side lobes of higher level signals. They cannot be handled like standard scatterers and present completely different geometric behaviour not related to their position in the radar image. This paper discusses the way to identify those artifacts and analyses their impact on SPN measurements compared to their reference points (centre of the main lobe).

1. INTRODUCTION

SPN is a PSI technique which has as its main scope displacement measurement over all the pixels in the radar image [1,2]. It has as main inputs an initial mask of stable points and an appropriate set of differential interferograms. The initial selection of stable points can be obtained by several ways depending on the number of available SAR images and on the desired spatial resolution for the processing. Then, the amplitude stability of every pixel on the SLC's can be exploited for high resolution SPN analysis when a large number of images are available [3]. In the same way a stacking of interferometric coherence can be used when SPN runs in medium and/or low resolution or when the available number of images are reduced (typically less than 20).

$$\Phi_{INTERF} = \Phi_{TOPO} + \Phi_{MOV} + \Phi_{APS} + \Phi_{NOISE} \qquad (1)$$

SPN is based on an interferometric phase model adjustment, Eq. 1. This is done iteratively, firstly over the initial mask of stable points and finally in a pixel by pixel manner. The model coherence gives a quantitative indication of the quality of this phase model adjustment in a stacking of N interferograms, see Eq. 2.

$$COH = \left|\sum_{i}^{N} e^{j(\Phi_{DInSAR\_i} - \Phi_{model\_i})}\right| / N \qquad (2)$$

However some pixels have an artificial nature since they are originated by Synthetic Aperture Radar processing itself. Those artifacts appear in positions of the radar image giving information not related with the real terrain associated to those pixels. The impact of two particular SAR artifacts in subsidence SPN measurements will be discussed in this paper.

2. INTRODUCTION TO AMBIGOUS SPN MEASUREMENTS

Two particular SAR artifacts are considered in this paper, azimuth ambiguities and range side lobes. The origin of those two artifacts will be explained briefly in this chapter. Some particular characteristics will be remarked in order to study their impact on PSI interferometry.

2.1. SAR azimuth ambiguities

Azimuth ambiguities are originated by the SAR signal undersampling in azimuth together with the length of the azimuth response given by the azimuth antenna pattern. The signal received, which is weighted by the azimuth antenna diagram has a Doppler spectrum wider than the PRF, so the Nyquist sampling rate is not kept. Those frequencies higher than the PRF coming from the side lobe regions of the azimuth antenna are folded into the main part of the signal spectrum centred on the image Doppler centroid (which corresponds to the main

Proc. 'Envisat Symposium 2007', Montreux, Switzerland
23–27 April 2007 (ESA SP-636, July 2007)

lobe of the antenna) so that aliased signals are produced giving origin to ambiguous responses. In the SAR image azimuth ambiguities appear displaced predominately in azimuth since they are observed a multiple of the integration time before and after the main response is acquired. However they are also displaced in range since the range migration curve of the ambiguous response is different from the one of the main response, Eq. 3.

$$x_i = \frac{\lambda \cdot r_0}{2 \cdot V} \cdot \left(PRF \cdot i - f_{DC} \right) \quad r_i = \frac{x_i^2}{2 \cdot r_0} \qquad (3)$$

- x_i azimuth displacement
- r_i range displacement
- λe st system wavenumber
- r_0 shortest near range sensor to target
- V sensor velocity
- f_{DC} Doppler frequency
- i ambiguity number

From Eq. 3 it can be inferred that this displacement depends mainly on the particular image acquisition conditions and acquisition mode timeline. Typical values for both displacements in the case of ERS-2 satellite are around 5600m in azimuth and 18.5m in range. Then, for similar Doppler rates in an image stacking of the same track the relative position of these ambiguities in azimuth and in range can be calculated. An example can be seen in Fig. 1 for a stacking of 31 ERS1/2.

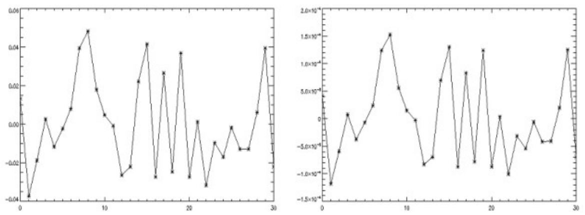

a) b)

Figure 1. Pixel relative positions of an azimuth ambiguity in azimuth (a) and in range (b) versus its main target for a stacking of 31 ERS1-2 images.

In Fig. 1 it can be seen that the position of the azimuth ambiguity remains extremely stable over the SLC's, at least under the expected coregistration precision (which is around 0.15 pixel). Furthermore, and following the literature, azimuth ambiguities appear slightly unfocused and their phase values are the same as for the main target [4,5]. Following these considerations the selection of azimuth ambiguities as Persistent Scatterers with a strong reflectivity could be an issue.

2.2. Range side lobes

The use of chirp signals in spaceborne SAR systems allows a substantial reduction in the peak transmitted power of a radar without reduction of signal-to-noise ratio (SNR). In pulsed radar, a long duration, high bandwidth signal is transmitted. The received data is compressed by applying a match filtered, by correlating it with a reference function, usually a replica of the transmitted chirp signal. Thanks to this operation targets coming from different echoes can be detected from an apparent noisy signal. The resulting time domain waveform for those targets is a sinc function. Its disadvantage is the presence of side lobes. This results in unsatisfactory performance since low level signals can be masked by the side lobes of higher level signals. The width of the main lobe corresponds to redundant information with respect to the centre of the target response while side lobes express position uncertainty.

Thus, side lobe weighting can be introduced at the processing level in order to overcome this problem. The most widely used weighting function is the Hamming window, at the cost of geometrical resolution degradation. Other methods could be used such as SVA [6] which presents a good trade-off between side lobes reduction and geometrical resolution preservation. However the effect of such a technique in interferometric applications is not yet fully assessed.

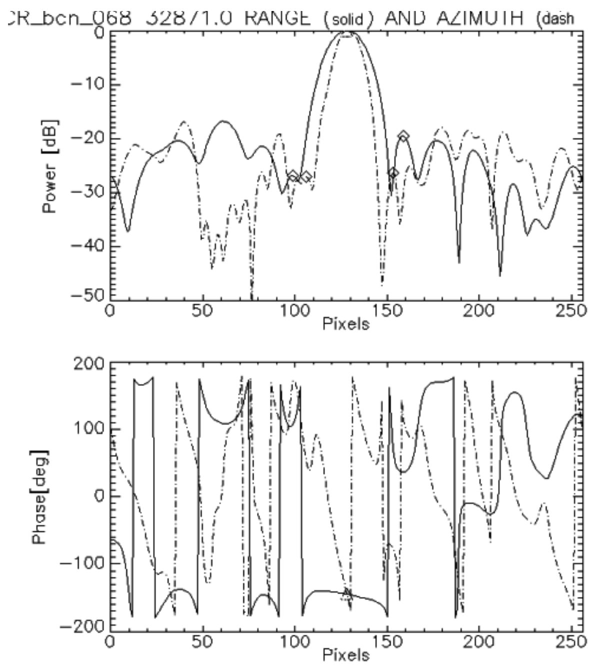

Figure 2. Example of amplitude (above) and phase (below) Impulse Target Response function for a strong target in the image.

It is important to remark that range main lobe and secondary lobes follow the properties of strong radar targets impulse response: stable phase in range and a ramp in azimuth in function of the image Doppler centroid. This can be checked in the IRF of a real strong scatterer presented in Fig. 2.

3. IMPACT ON SPN MEASUREMENTS

These two SAR artifacts give ambiguous information at two different scales. Replicas of strong targets appear about 5600 meters away from the main target in the SAR image. Meanwhile range side lobes are close to the main target masking the response of neighbours low-backscattering pixels.

The impact of these artifacts on SPN measurements will be analysed in function of the SPN steps at where they could be included as Stable Point. Thus, considering when they can give SPN coherent measurements unrelated to the real focused area associated to those radar pixels. So the analysis can be classified as

- selection of ambiguous pixels as initial mask of stable points
- selection of ambiguous pixels as final coherent SPN points of displacement measurement.

3.1. SAR azimuth ambiguities in SPN measurements

Taking into account the theoretical studies exposed in chapter 2 the selection of ambiguous pixels within the initial mask of stable points is expected. To test if occurs two different SLC datasets are generated from a set of 31 ERS1-2 RAW data:

- By focusing the full azimuth band. Resulting in a noticeable presence of azimuth ambiguities clearly visible in dark areas of the image.
- By focusing with 80% of the azimuth band (cutting the 20% of the band considering the image Doppler centroid frequency, which is optimum for ambiguity reduction in ERS1-2 & ASAR IS2 mode). Resulting in a considerable reduction of the azimuth ambiguities.

Then by differentiation of the multi-mean reflectivity images resulting from each dataset azimuths ambiguities can be perfectly distinguished and localised, see Fig. 3 for an example.

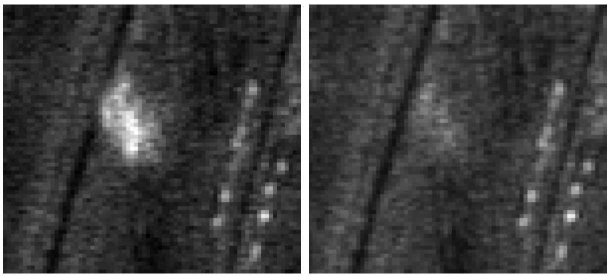

a) b)

Figure 3. Example of Multi-mean reflectivity image in a low-backscattering area with the SLC's focused by taking the full azimuth band (a) and only 80% (b). The average multi-mean pixel values for azimuth ambiguities are around 0.6.

Two different masks of stable points are obtained by exploiting the amplitude stability of the SLC's pixels in both stacking of 31 images. Almost 90% of the initial stable points are common. These have an identical mean reflectivity in both datasets. The remaining 10% of non-common stable points have a very similar mean-reflectivity value. The ones with the higher differences are due to changes in the amplitude level of part of the azimuth main lobe of high-level targets. This is a normal effect considering that the azimuth spectrum was cut, so this is translated into a spread lobe effect in the slow-time domain.

For this particular test case no azimuth ambiguity pixels were selected as stable point. Deeper analysis can be driven by looking at the IRF of a strong and very stable target and its azimuth replicas in low backscattering areas. An example is shown in Fig. 4.

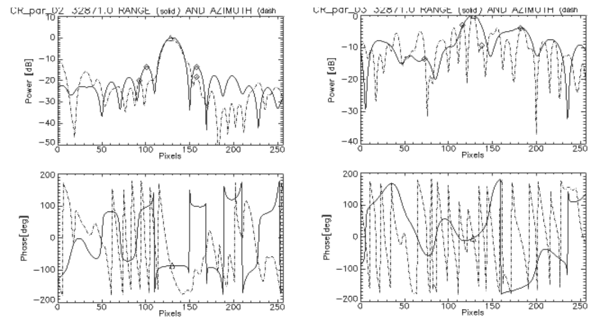

a) b)

Figure 4. Example of IRF for a strong and stable target (a) and its first azimuth replica (b) not selected as stable point by means of multi amplitude stability analysis.

From Fig. 4 it can be observed that the background as a considerable impact on the ambiguity. In general as illustrated in Fig. 4 (a), although the real target as a peak to clutter ratio sufficiently high to be well discriminated, the ambiguity is closer to the background level Fig. 4 (b), due to the simple azimuth antenna pattern weighting

[5]. As the background is changing with the temporal conditions (wind, moisture, seasons), it results in an amplitude fluctuation hiding more or less the ambiguity along the temporal SLC data stacking. It can also be observed that the background impacts the ambiguity phase as it is not the same as the main target while theoretically they should be the same target [4,5]. In any case, the spatial phase behaviour of the ambiguities is the same as for strong targets, but as it was said, with a different phase value versus its main target.

From an interferometric point of view, this behaviour is translated into good coherence in DinSAR phases. Then on a stacking of interferometric coherence azimuth ambiguities could be selected within a mask of initial stable points. See figure 5 for an example.

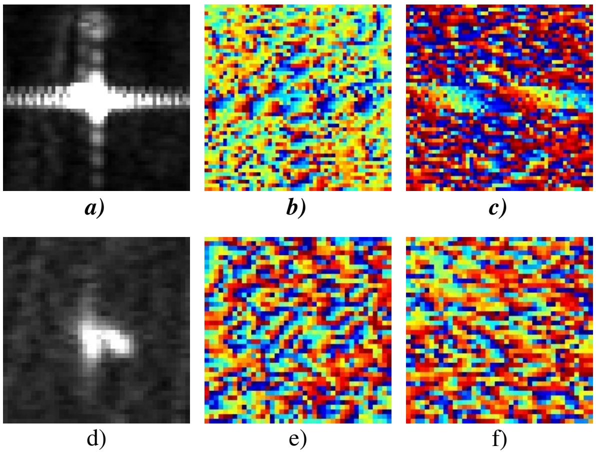

Figure 5. Example of DInSAR fringes for a real target (a,b,c) and for its azimuth ambiguity (d,e,f). Multi mean image for the real target (a) and for the azimuth ambiguity (d). Interferometric phase with height of ambiguity of 40 meters for the real target (b) and for the azimuth replica (e). DInSAR phase with a height of ambiguity of -100 m for the main target (c) and for the azimuth ambiguity (f).

However, instead they have interferometric coherence azimuth ambiguities are not properly modelled under SPN. Their interferometric phases do not follow any particular pattern in baseline, Doppler or time. Their behaviour are similar to any other noisy pixel, see Fig. 6 for an example baseline first order modelling.

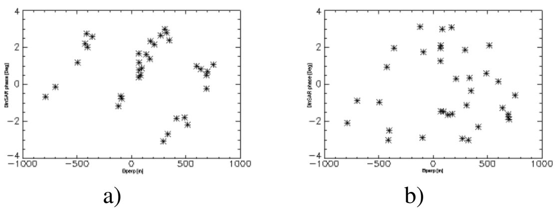

Figure 6. Example of InSAR phase stacking in function of the perpendicular baseline for a real target (a) and for the azimuth ambiguity (b).

This reveals that the interferometric phase of those ambiguous pixels is corrupted by these three reasons:

- The phase value is not the same as for its main target response in the SLC image with a real background clutter.
- The local topography used when producing the DInSAR phases is not correct for the ambiguity (they are located 5600 m away from its real position).
- Likewise for the pixels' atmospheric compensation within SPN.

In conclusion azimuth ambiguities are not selected as final SPN points of measurements because their stacking of DInSAR phases can not be properly modelled. Due to different phase model mis-compensations the stacking of the ambiguity phases do not follow any particular pattern.

3.2. SAR side lobes in SPN measurements

Main lobes and side lobes of strong targets are selected as stable points based on the SLC's amplitude stability as well as on the mean interferometric coherence. Therefore it is a problem that should be considered in SPN since it is found from the beginning of the process.

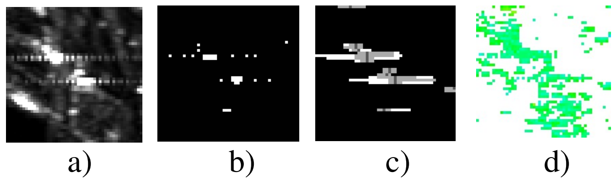

Figure 7. Example of range side lobes inclusion in SPN analysis. a) Multimean amplitude image. b) initial mask of stable points by means of SLC's amplitude stability. c) side lobes and secondary lobes pixels detection. d) consistent final subsidence rate measured in side lobes.

As it was said in chapter 2 range side lobes have a particular phase behaviour in relation with the centre of the main lobe. They have a constant phase value in range and follow a ramp in azimuth based on the Doppler centroid characteristics of the SLC, see Fig. 4. Thanks to this particular geometrical behaviour their interferometric phases can be modelled within SPN in order to set the effective spread of the signal response for strong targets. Side lobes pixels coming from strong and coherent targets can be identified and classified. After that their phases can be compensated allowing to measure the same displacement in SPN.

In Fig. 7. an example of side lobes inclusion in SPN analysis is given. It can be seen how part of main lobes and secondary lobes of strong targets are included in the initial selection of stable points for an SPN processing, Fig. 7.a and 7.b. Then based on the geometrical phase behaviour of the side lobes the spread of the signal response can be set, Fig 7.c. Pixels included within the same target response can be identified and classified as centre of the main lobe (dark grey in Fig. 7.c), part of the main lobe (light grey in Fig. 7.c) and secondary lobes (white in Fig. 7.c). Thanks to this geometrical phase model the SPN subsidence measured is consistent for all range side lobes as it can be observed in Fig. 7.d.

However this subsidence consistency must be checked properly for the whole studied area. In Fig. 8 the histogram of the subsidence rate difference measured by the centre of the target and by the range side lobes can be observed. The histogram is showing that effectively the measured rate is the same. The observed width of 0.1 cm/years in the subsidence difference is due to the higher level of noise that can be found in side lobes.

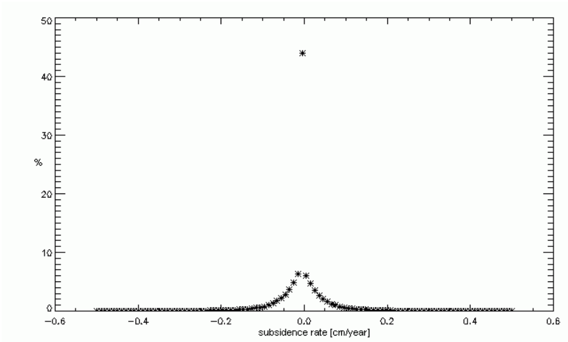

Figure 8. Histogram with the mean subsidence rate difference between the centre of the target and the range side lobes for all the strong and coherent target of an area of 500 Km^2.

Consequently there is no reason for keeping all these redundant points in the final SPN selection. They are synthetically produced from the signal response of strong scatterer and they do not represent any new information. Moreover they have more phase noise which is translated into more fluctuations when looking at their displacement time evolution. By removing these ambiguous points there are two main improvements in SPN subsidence measurements:

- efficiency in the quantity and in the quality of the final selected points. In an area of about 500 Km^2 there is an optimisation of a 30% in the final number of good points without loss of information.
- precise final ground position of the measurements. Produced by reducing the position uncertainty introduced by the fact of having so many replicas of the same point spread along the projection of the satellite line of sight onto the ground

In Fig. 9 those improvements can be observed in a graphical way. It this figure it can be observed how the subsidence measured in the side lobes is consistent with the value given by centre of the target response. Moreover it can be appreciated visually the improvement achieved in the final location of the measurements by removing the redundant scatterers given by the side lobes.

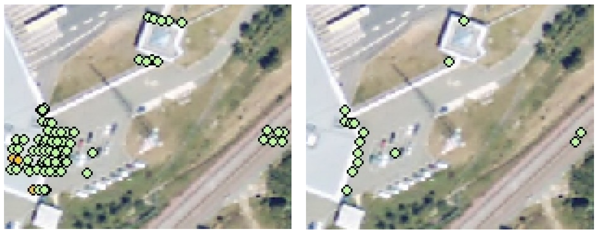

a) b)

Figure 9. Example final geocoded SPN mean rate subsidence. a) result of a normal geocoded final selection based on the SPN model coherence. b) improved final selection considering only the centre of the main lobe for strong scatterers.

4. CONCLUSIONS

Preliminary results regarding the evaluation of the impacts of two particular SAR artifacts on PSI subsidence measurements was presented in this paper. The study was based on the analysis of the behavior of azimuth ambiguities and range side lobes in an stacking of SLC's and interferograms and their impact on subsidence estimates.

Azimuth ambiguities appear incoherent in a stacking of images. Their stacking of DInSAR phases do not present any particular pattern so they can not be properly modelled within SPN. One possible explanation is the coherent interaction of the ambiguity response with its image background because of the low signal to noise ratio. For the analysed test cases no ambiguity pixel was selected as a final point of good displacement measurement. However, further analysis must be carried out for ambiguities of extremely strong and coherent scatterers over areas with very low backscattering.

Range side lobes are selected as stable points as they are presenting coherent phase behaviour in a stacking of SLC's. The width in pixels of the range response for strong targets can be set. Then side lobes displacement estimates were compared to the those of in the centre of the main lobe obtaining consistent results. It was demonstrated that side lobes are introducing information redundancy and uncertainty in the geocoding of the final estimates. By taking only the centre of the main lobe as a good point of measurement improvements in terms of information efficiency and precise geocoding can be achieved. Further studies will be carried out in dense urban areas where strong and coherent scatterers are presented in close proximity to each others with a high risk of interferences.

6. REFERENCES

1. J. Duro, J. Inglada, J. Closa, N. Adam, A. Arnaud, "High Resolution Differential Interferometry using time series of ERS and ENVISAT SAR data" ENVISAT Symposium, Salzburg, Sept 2004.
2. J. Duro, M. Sanchez, N. Miranda, G. Cooksley, A. Arnaud, "SPN examples of subsidence monitoring and validation" 7ª Semana de la Geomatica, Barcelona, Feb. 2007
3. A. Ferretti, C. Prati, F. Rocca, "Analysis of Permanent Scatterers in SAR Interferometry" IGARSS 2000, Honolulu, Jul. 2000.
4. A. Moreira, "Suppressing the azimuth ambiguities in synthetic aperture radar images", IEEE trans. geosci. remote sensing, vol. 31, No. 4, july 1993
5. A. Monti Guarnieri, "Adaptive removal of azimuth ambiguities in SAR images", IEEE trans. geosci. remote sens. 2005, vol. 43, no3, pp. 625-633
6. J. Fischer, I. Pupeza, R. Scheiber, "Sidelobe Suppression Using the SVA Method for SAR Images and Sounding Radars", EUSAR 2006, Dresden, May 2006.